UC Irvine
UC Irvine Previously Published Works

Title

Radiometric surface temperature measurements during dye-assisted laser skin closure: In vitro and in vivo results

Permalink

https://escholarship.org/uc/item/0pr2m2tf

Journal

Lasers in Surgery and Medicine, 25(4)

ISSN

0196-8092

Authors

Fried, Nathaniel M
Choi, Bernard
Welch, Ashley J
et al.

Publication Date

1999

DOI

10.1002/(sici)1096-9101(1999)25:4<291::aid-lsm4>3.0.co;2-#

Copyright Information

Peer reviewed

Radiometric Surface Temperature Measurements During Dye-Assisted Laser Skin Closure:
In Vitro and In Vivo Results

Nathaniel M. Fried, PhD,[1]* Bernard Choi, MS,[2] Ashley J. Welch, PhD,[2] and Joseph T. Walsh, Jr., PhD[1]

[1]Biomedical Engineering Department, Northwestern University, Evanston, Illinois 60208
[2]Biomedical Engineering Program, The University of Texas at Austin, Austin, Texas 78712

Background and Objective: A thermal camera was used to measure surface temperatures during laser skin welding to provide feedback for optimization of the laser parameters.
Study Design/Materials and Methods: Two-centimeter-long, full-thickness incisions were made in guinea pig skin in vitro and in vivo. India ink was applied to the incision edges, which were then mechanically apposed. Continuous-wave, 1.06-μm Nd:YAG laser radiation was scanned over the incisions, producing an effective pulse duration of ~100 msec. Cooling durations between scans of 1.6, 4.0, and 8.0 sec were studied in vitro. A 5-mm-diameter laser spot was used with the power kept constant at 10 W. Thermal images were obtained at 30 frames per second with a thermal camera detecting 3–5 μm radiation. Surface temperatures were recorded at 0, 1, and 6 mm from the center line of the incision.
Results/Conclusions: Cooling durations of 1.6 and 4.0 seconds in vitro resulted in temperatures at the weld site that remained above ~65°C for prolonged periods of time. Cooling durations of 8.0 seconds were sufficient both in vitro and in vivo to prevent a significant rise in baseline temperatures at the weld site over time. Lasers Surg. Med. 25:291–303, 1999.   © 1999 Wiley-Liss, Inc.

Key words: tissue welding; thermal camera; infrared radiation

INTRODUCTION

In previous studies of laser skin closure, pulsed radiation that was strongly absorbed by a dye coating the incision edges produced strong welds with limited thermal damage to surrounding healthy tissue [1–2]. Histologic analysis and tensile strength measurements were used to optimize the large number of laser parameters involved in tissue welding. This study examines the use of surface temperature measurements as a third source of information for optimizing the welding parameters.

The majority of previous laser skin closure studies have used either continuous-wave (CW) delivery of radiation [3–7] or temperature-controlled photocoagulation systems [8] to weld tissue. Temperatures were maintained above the thermal damage threshold of skin for extended periods of time, resulting in heat diffusion from the weld site into surrounding tissue and, as a consequence, a zone of lateral thermal damage on the order of 500 μm or greater. A large zone of

thermal damage may result in a significant amount of scarring during wound healing and therefore may be unacceptable for skin closure applications.

The objective of our scanning welding technique is to deliver the radiation selectively to the weld site in a series of sufficiently short pulses, with adequate cooling between scans, to achieve selective cumulative thermal denaturation at the weld site and avoid unnecessary thermal damage to adjacent tissue. Both temporal and spatial temperature information provide indicators of the extent of damage that will occur due to thermal denaturation of collagenous tissue.

It should be mentioned that the threshold of tissue denaturation is a function of heating time and of temperature. As the heating time decreases, the threshold temperature necessary to denature tissue increases. An Arrhenius model is typically used to determine the amount of thermal damage incurred for a certain time period in which the tissue is kept at a constant temperature. During a 100-msec exposure, for example, Moritz and Henriques [9] determined that thermal damage in skin occurred at ~63°C. Another study by Weaver and Stoll [10] found a thermal damage temperature of ~67°C. In the present study, a temperature of 65°C was used as a reference for the thermal damage threshold in skin.

Temperature measurements provide several important pieces of information to assist in the optimization of the scanning welding technique. First, during pulsed welding, it is necessary to allow the temperature at the weld site to cool approximately to initial prewelding temperatures between successive pulses. Thus, the baseline temperature does not rise above the thermal damage threshold. Temperature data will allow one to estimate the cooling time between scans necessary to minimize an accumulation of thermal energy. Optimization of the cooling time will not only prevent unnecessary thermal damage in the tissue surrounding the weld site, but by eliminating unnecessary cooling time, the total operation time may also be reduced, thus making welding more competitive with other tissue closure techniques.

Second, it is necessary to achieve peak temperatures above the thermal damage threshold to obtain a sufficient amount of thermally denatured tissue at the weld site for strong welds to develop. Thus, the temperature measurements during an individual scan will help determine the irradiance necessary to produce peak temperatures above the tissue denaturation threshold. Third, the temperature data will help determine the number of laser pulses, or total energy, needed to denature tissue at the weld site. Fourth, temperature data can be correlated with visual cues of tissue denaturation, heat diffusion models, and thermal denaturation models to assist in the optimization of all of the laser parameters.

It should be emphasized that the goal of this study was not to determine a temperature endpoint for laser skin welding but rather to produce data that will help optimize the laser parameters (irradiance, radiant exposure, pulse duration, and cooling between pulses).

MATERIALS AND METHODS

In Vitro Experiments

For the in vitro temperature measurements, a procedure described by Fried and Walsh was used [1]. Adult female albino guinea pigs (age = 7–8 weeks, weight = 400–500 g; Harlan, Indianapolis, IN) were anesthetized with halothane (Halocarbon Laboratories, River Edge, NJ) and then euthanized with an intracardiac overdose of sodium pentobarbitol (Nembutal, Abbott Laboratories, North Chicago, IL). Animals were shaved and then epilated with a chemical depilator (Nair, Carter-Wallace, New York, NY). The dorsal skin, including epidermis and dermis, was excised with a scalpel and sectioned into squares of approximately 3 cm × 3 cm. Tissue samples were then enclosed in a Petri dish and preserved on a saline-soaked towel until used. All experiments were completed within 12 hour of tissue preparation.

A 2-cm-long, full-thickness incision was made in each skin sample with a no. 15 scalpel. Approximately 2–5 µl of India ink (~100-nm particle diameter; Black India Rapidograph Ink, 3080-F, Koh-I-Noor, Bloomsbury, NJ) was then applied to the wound edges with a micropipette. India ink was chosen for this study because its high absorption coefficient limits radiation absorption to the immediate area of the weld site; it has broadband absorption, thus obviating the need for a laser emitting at a specialized wavelength; it is biocompatible; and it is readily available. Excess dye was removed from the wound edges with a paper towel. After the India ink dried, a thin layer of egg white (10% albumin) was applied to the wound edges as a temporary adhesive.

Welding was performed with a CW Nd:YAG

laser (Model 703T, Lee Laser, Orlando, FL) emitting radiation at a wavelength of 1.06 μm. At this wavelength, the radiation penetrates several millimeters into the tissue, thus making it possible to achieve deep, full-thickness welds in skin. The radiation was coupled into 600-μm-core-diameter silica optical fibers (Thor Labs, Newton, NJ) for flexible delivery. A 5-mm-diameter (FWHM) laser spot was maintained during the experiments. A large laser spot diameter, much greater than the ~2-mm-thick skin, is necessary to reduce attenuation of the laser beam in the subsurface layers of the tissue due to light scattering and thus to provide the most uniform heating of the weld site with depth. The beam profile, as measured by scanning a 200-μm-diameter pin hole across the beam, was approximately Gaussian. The power delivered to the tissue was measured by a power meter (Molectron PowerMax 5100, Portland, OR) prior to each weld; the power was kept constant at 10.0 ± 0.2 W for all experiments. The fiber was scanned back and forth along the axis of the weld site by using a stepper-motor-driven translation stage (Newport, Irvine, CA) to simulate pulsed delivery of the radiation. The stepper motor was controlled by a personal computer (Hewlett Packard 386, Palo Alto, CA) that allowed programming of the scan velocity, cooling time between scans, and total number of scans. During welding, the velocity of the translator was kept constant at 47.6 mm/second, resulting in a line scan time of 0.42 second and an effective pulse duration, τ_p, of ~100 msec, for the fixed 5-mm-diameter laser spot. A laser pulse duration of ~100 msec was chosen to limit thermal diffusion during the laser pulse to a lateral zone of ~220 μm from the weld site. Previous studies have shown that, if the thermal damage zone is much greater than ~200 μm, then the amount of scarring increases significantly during wound healing [11,12].

The cooling time between scans was changed to study the superposition of temperature by successive scans. Three cooling times were selected: τ_c = 1.6, 4.0, and 8.0 seconds. The short cooling times were intended to represent quasi-CW delivery of radiation in which the temperatures at the weld site remained above collagen denaturation temperatures for prolonged periods of time. The intermediate cooling times were intended to allow the weld site to cool below collagen denaturation temperatures between laser pulses. The long cooling times were intended to allow the weld site to cool to approximately its initial temperature between laser pulses, thus preventing a buildup in the baseline temperature above collagen denaturation temperatures with the application of successive pulses. The cooling time was defined as the average time the laser beam took to return to a particular 5-mm spot at the weld site during scanning. For example, for the 1.6-second cooling time, the incision ends were cooled at either 1.2 or 2.0 seconds, depending on the scan direction. The temperature data, however, were collected at approximately the incision midpoint where the cooling time was independent of scan direction. Between scans, the laser beam was incident on high-reflecting metal plates placed on either side of the tissue sample. Each scan delivered 4.2 J of total energy to the incision, and so the total energy delivered to the incision was ~300 J delivered in 70 passes. The average fluence per scan at any particular point along the incision was 5.1 J/cm². The total operation time varied between 3 and 10 minutes, depending on the cooling time between scans. Table 1 provides a summary of the laser parameters used in the in vitro experiments.

Thermal images were recorded at 30 frames per second with a 3–5-μm band-limited HgCdTe thermal camera (Model 600L, Inframetrics, North Billerica, MA). The field of view was 3 cm × 3 cm with a 24.13-cm working-distance, close-up lens. The spatial resolution of the thermal camera was approximately 120 μm per pixel. The mean temperature resolution in the 20–120°C range was 0.4°C. The emission of the sample was assumed to be 1.0 [13]. Gray-scale images were recorded on videotape using a Super VHS video recorder (Panasonic, Tokyo, Japan). The translation stage, which scanned the optical fiber across the weld site, was placed between the camera and the weld site. The camera was placed at an angle of approximately 5–10° with respect to the weld site to prevent the optical fiber from blocking the field of view of the camera during welding, but because the camera was shielded when the fiber passed in one direction, data were taken only once every other scan.

Surface temperature measurements were taken at three points: on the axis of the weld site, where the ink-stained tissue was directly heated; 1 mm off axis, where the tissue was partly heated; and 6 mm off axis, where the tissue was not directly heated. Because of the large amount of data to be processed, data points were selected for analysis in intervals of six scans. Frames of interest were acquired by using a frame grabber (Scion Corp., Frederick, MD) and a dedicated imaging computer (Macintosh IIfx, Apple, Cupertino, CA)

TABLE 1. Summary of Welding Parameters

Parameter	In vitro	In vivo
Incision length:	2 cm, full thickness	
Laser:	Continuous wave Nd:YAG	
Wavelength:	1.06 μm	
Power to tissue:	10.0 ± 0.2 W	
Dye:	India ink	
Absorption coefficient:	3,500 cm^{-1}	
Scan speed (mm/sec)	47.6	47.6
Pulse duration (msec)	100	80
Cooling time (sec)	1.6, 4.0, and 8.0	8.0
Spot diameter (mm)	5 (FWHM)	4 (FWHM)
Number of scans	70	75
Total energy (J)	300	315
Fluence (J/cm^2)	5.1	6.7
Operative time (min)	3–10	10
Adhesive	Egg white (10% albumin)	clamps

and were processed by using the Image 1200 image software package (Scion Corp.). Gray-scale values were converted to temperatures by using calibration algorithms in Matlab 5.1 (MathWorks, Natick, MA) that were specific to the thermal imaging system used in these experiments. Two samples were taken for each set of parameters. All data were plotted as the mean value ± the standard deviation (SD) of the population.

In Vivo Experiments

Some of the laser parameters were changed when progressing from the in vitro to the in vivo experiments in an effort to anticipate the cooling effects of perfusion and hydration at the weld site during in vivo welding. Specifically, the fluence was increased from 5.1 J/cm^2 to 6.7 J/cm^2 to compensate for cooling due to perfusion and increased hydration of the tissue. Because the laser was already operating at maximum power, it was necessary to decrease the laser spot size from 5 to 4 mm to obtain the higher fluence level. It should be emphasized that when a scanned CW laser is used to simulate pulsed delivery of radiation, the pulse duration, spot size, and fluence are no longer independent laser parameters. When one parameter is adjusted, the other parameters also change. Despite this limitation, we felt that a scanned laser beam provided additional advantages over a mechanically chopped, pulsed laser system, such as a smoothing out of inhomogeneities in the laser beam profile and a more uniform delivery of the radiation over the weld site.

The following procedure was used for the in vivo experiments, as described by Fried and Walsh [2]. The guinea pigs were shaved and then epilated with a chemical depilator. Each guinea pig was anesthetized with atropine (0.05 mg/kg), ketamine (30 mg/kg), and xylazine (2 mg/kg) administered by intraperitoneal injection. One percent lidocaine with 1:100,000 epinephrine was used as a local anesthetic at each incision site. Two-centimeter-long, full-thickness incisions were made parallel to the spine with a no. 15 scalpel. Approximately 2–5 μl of India ink was applied to the wound edges with a micropipette. The ink was allowed to dry, and excess ink was removed with cotton swabs. The anesthetized animal was then placed on its side on a stage. A mechanical clamping system was used to grip and push the wound edges together. After the procedure, the anesthetized guinea pig was euthanized with an intracardiac overdose of sodium pentobarbitol (Nembutal, Abbott Laboratories).

For the in vivo experiments, a 4-mm-diameter (FWHM) laser spot was maintained during the experiments. The power was kept constant at 10.0 ± 0.2 W. An effective pulse duration of ~80 msec was used with 8.0 seconds of cooling between scans. Operation time was kept constant at 10 minutes per incision. The total energy delivered to the weld site was approximately 315 J, delivered in 75 scans. These parameters were chosen based on the best results from previous experiments performed in vitro, in which both histologic measurement of thermal damage and tensile strength results were used to optimize the total energy (or number of laser scans) and the cooling time between scans [1]. Each scan delivered 4.2 J of energy to the weld site. The average fluence per scan at any particular point along the incision was 6.7 J/cm^2. Table 1 provides a summary of the laser parameters used in the in vivo experiments. To minimize thermal damage to the
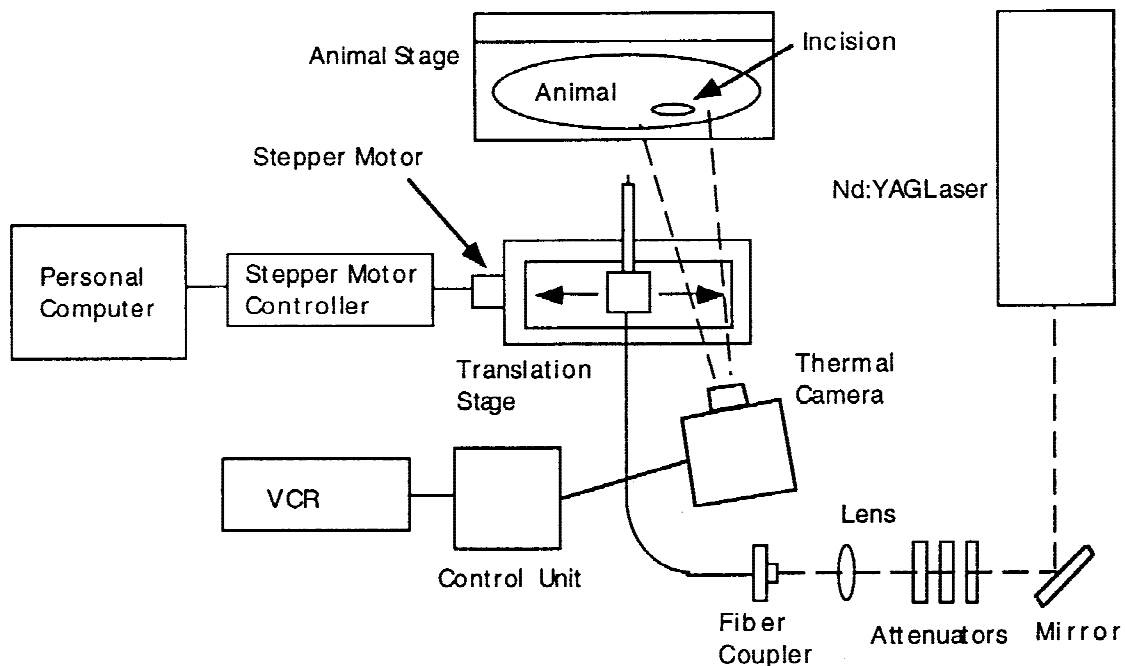
Fig. 1. Experimental setup for temperature measurements during laser skin welding.

skin beyond the incision ends, the beam was blocked with high-reflecting metal plates placed on each end of the incision. Figure 1 shows the experimental configuration used to record temperature measurements during in vivo welding.

RESULTS

In Vitro Surface Temperature Measurements

Figure 2A shows a graph of the peak surface temperatures for welding with short cooling times between pulses ($\tau_c = 16 \times \tau_p = 1.6$ seconds). The peak temperature is plotted as a function of lateral distance from the center of the weld site and time. The peak temperature rose to $104 \pm 6°C$ on the axis of the weld site. At 1 mm off axis, the peak temperature rose to $97 \pm 14°C$. The temperature at 6 mm off axis increased to $61 \pm 6°C$.

A representative time–temperature profile is plotted for an individual pulse, the 61st scan, in Figure 2B. Both on the axis of the weld site and 1 mm off axis, the temperature reached 110°C before falling to 83°C during the 1.6 seconds of cooling between scans. The temperature at 6 mm off axis reached as high as 67°C and remained at ~60°C during much of the cooling phase. At the weld site and 1 mm off axis, the temperature remained at or above the assumed thermal damage threshold (~65°C) for prolonged periods. This effect is similar to CW laser heating of tissue.

It should be noted that some of the temperatures measured at 1 mm off axis were slightly higher than those measured on the axis of the weld site. These errors in measurement can be attributed to gross changes (e.g. raising, curling) of the tissue sample with excessive heating, which affected the accuracy of the measurements.

Figure 3A shows a graph of the peak surface temperatures for pulsed welding with intermediate cooling times between pulses ($\tau_c = 40 \times \tau_p = 4$ seconds). For all three positions, the temperature continued to increase with successive pulses, reaching as high as $88 \pm 1°C$ on axis, $78 \pm 4°C$ at 1 mm off axis, and $54 \pm 3°C$ at 6 mm off axis. The surface temperatures rose well above the thermal damage threshold for both the measurements on axis and 1 mm off axis.

Figure 3B shows a representative graph of the time–temperature profile of a single pulse for the 61st scan. The temperature rose to 88°C at the weld site before falling to 62°C over a cooling period of 4 seconds. The temperature 1 mm off axis reached a peak of 82°C and then dropped to 59°C. At 6 mm from the weld site, temperatures remained in the range of 51–57°C. Four seconds of cooling between scans did not allow the tissue surface temperature at and near the weld site to drop significantly below the thermal damage threshold between successive pulses.

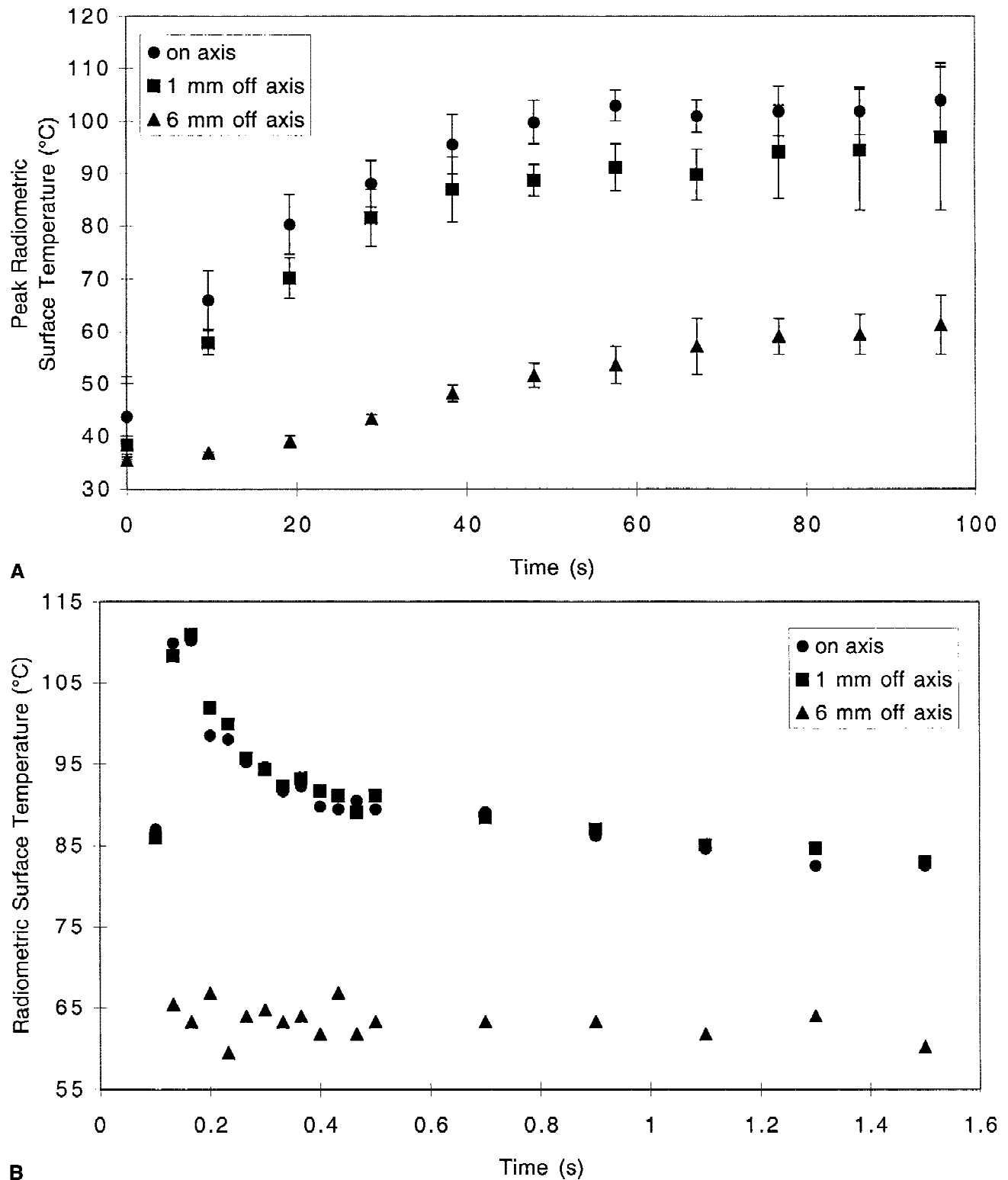The results shown in Figure 4, however,

A:

B

Fig. 2. **A:** Peak radiometric surface temperatures for welding in vitro as a function of time and distance from the weld site for 1.6 seconds of cooling between scans. Bars signify mean values ± SD (n = 2). **B:** Time–temperature profile for welding in vitro during the 61st scan with 1.6 seconds of cooling between scans.
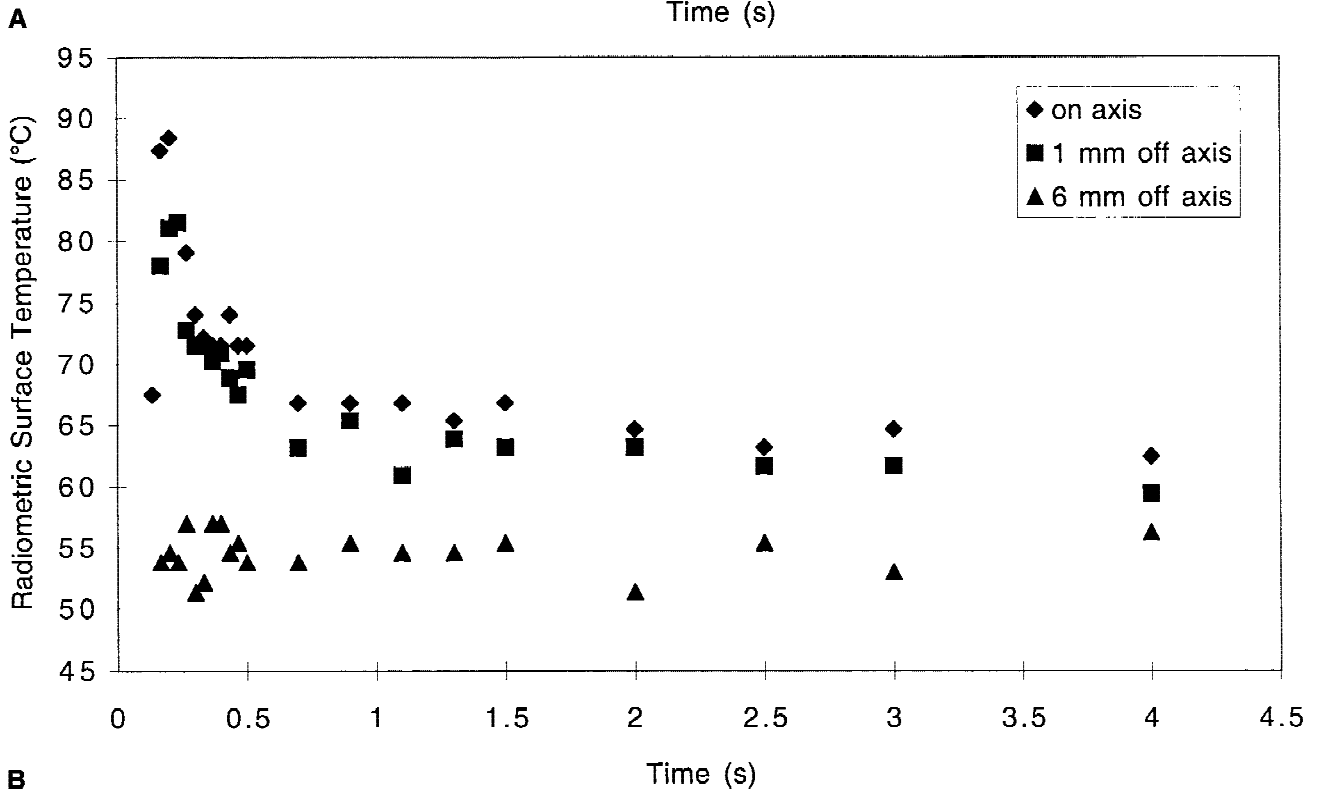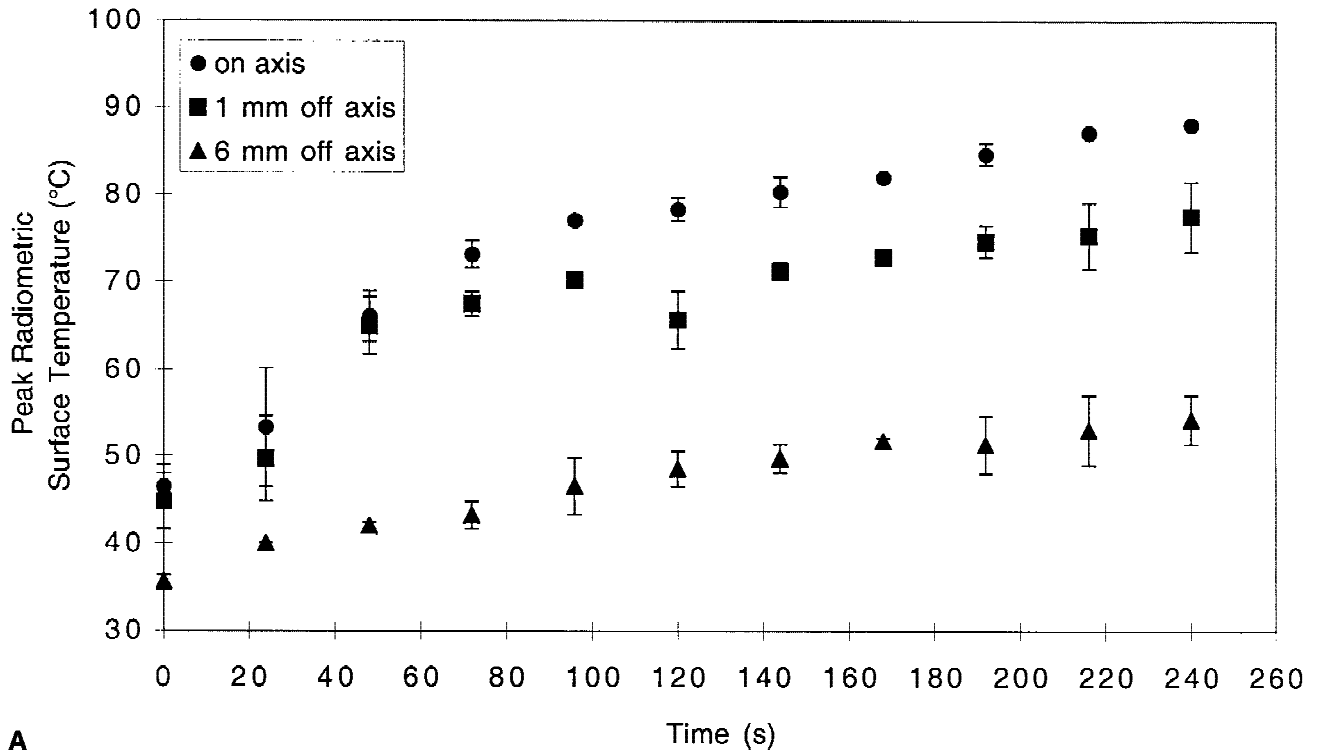
Fig. 3. **A:** Peak radiometric surface temperatures for welding in vitro as a function of time and distance from the weld site for 4 seconds of cooling between scans. Bars signify mean values ± SD (n = 2). **B:** Time–temperature profile for welding in vitro during the 61st scan with 4 seconds of cooling between scans.
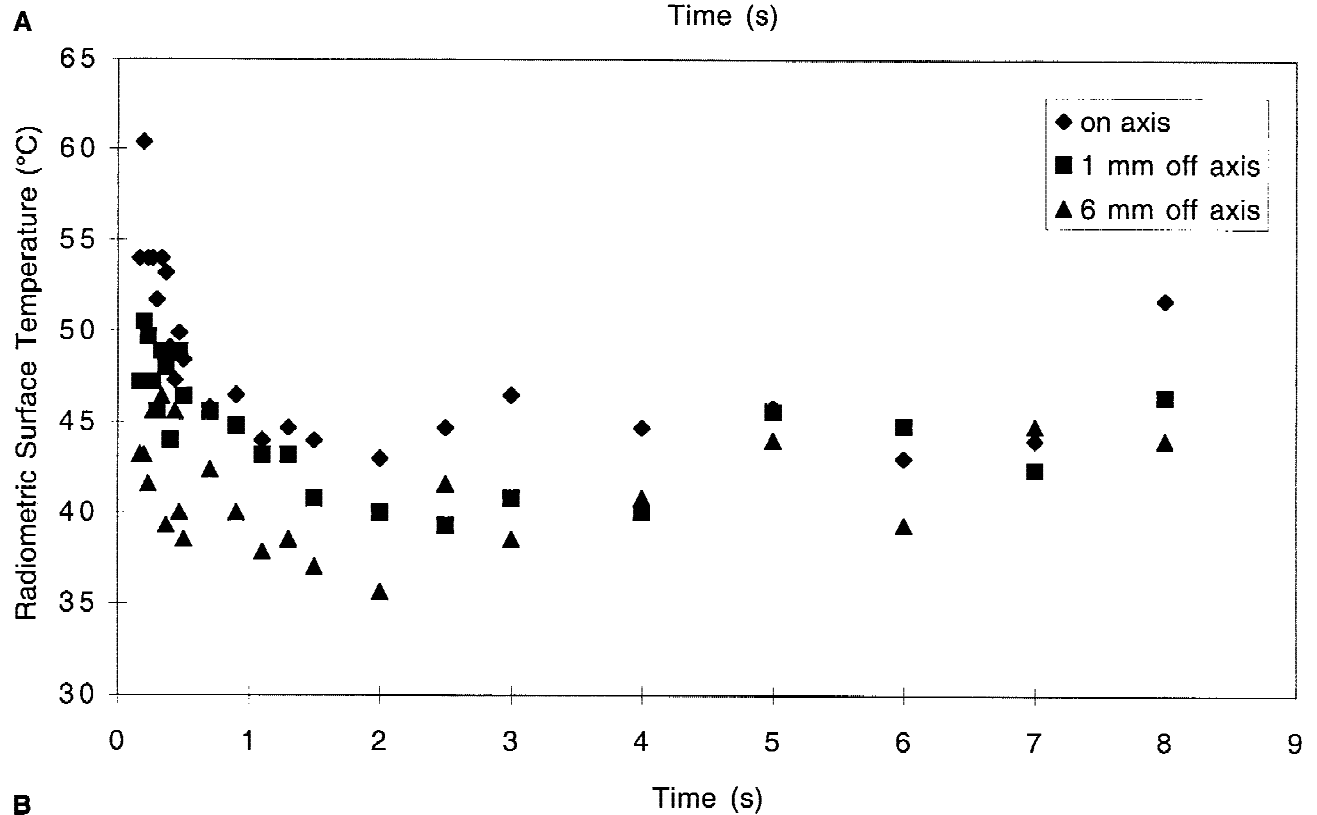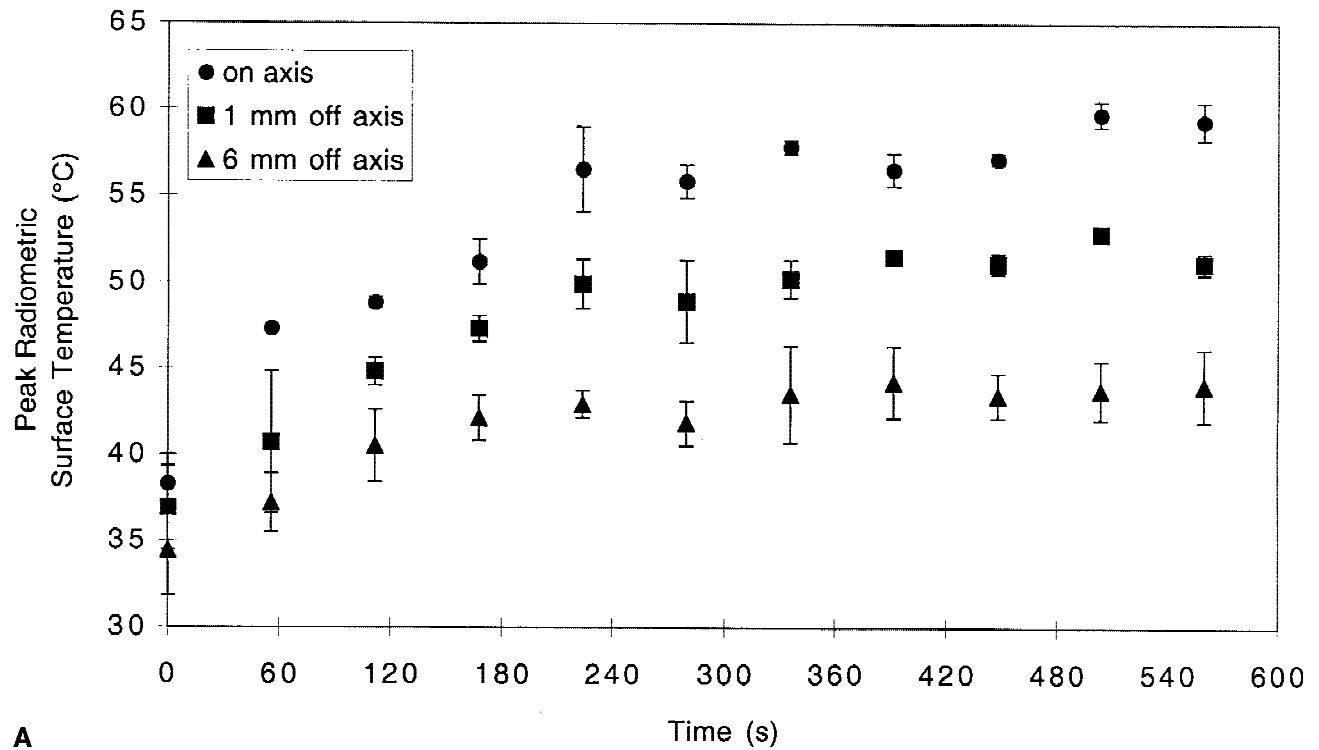
Fig. 4. **A:** Peak radiometric surface temperatures for welding in vitro as a function of time and distance from the weld site for 8 seconds of cooling between scans. Bars signify mean values ± SD (n = 2). **B:** Time–temperature profile for welding in vitro during the 61st scan with 8 seconds of cooling between scans.

significantly different temperature trends. Figure 4A shows a graph of the peak surface temperatures for welding with long cooling times between scans (τ_c = 80 × τ_p = 8 seconds). At the weld site, peak temperatures rose slowly, leveling out at 57 ± 1°C, after about 4 minutes of heating. The weld site was not excessively heated to peak temperatures ranging from 80–100°C, as occurred for short and intermediate cooling times. The tissue surrounding the weld site was held significantly below the thermal damage threshold. The surface temperature at 1 mm off axis leveled out and remained at 52 ± 1°C. At 6 mm away from the weld site, peak temperatures leveled out at 43 ± 1°C.

Figure 4B shows a representative graph of the time–temperature profile of a single pulse for the 61st scan. At the weld site, the temperature peaked at 60°C, around the thermal denaturation threshold, and then cooled to about 45°C after 8 seconds. At 1 mm off axis, the temperature peaked at 51°C and then dropped to approximately 43°C before the next pulse. The temperature at 6 mm off axis remained in the range of 36–44°C. Thus, there was no buildup in the baseline temperature above the thermal damage threshold with the application of successive pulses.

It should be mentioned that some of the temperatures measured at 6 mm from the weld site were slightly higher than those measured on the axis of the weld site. These differences occur at low temperatures after substantial cooling of the tissue. Although it is not clear why they appear, it is possible that "hot spots" in the ink layer due to nonuniform staining of the weld site caused irregular heating patterns in the tissue.

In Vivo Surface Temperature Measurements

Figure 5A shows a graph of the peak surface temperatures for pulsed welding with long cooling times (τ_c = 100 × τ_p = 8 seconds). The peak temperature at the weld site began to level off at 69°C. At 1 mm off axis, the temperature leveled off at 60°C. The temperatures at 6 mm off axis remained stable in the range of 39–41°C.

Figure 5B shows a representative graph of the time–temperature profile for a single pulse during the 61st scan. At the weld site, the temperature rose sharply to 70°C and then cooled quickly to about 45°C. The temperature at 1 mm off axis rose to 57°C and then also dropped to approximately 45°C. At 6 mm off axis, the temperature remained in the range of 32–40°C. Thus, temperatures were elevated above the thermal

damage threshold (~65°C) for short periods of time (~100 msec) and then cooled well below the threshold between pulses. This temperature rise was confined to the immediate area of the weld site.

Table 2 provides a summary of results for all of the temperature measurements. The maximum temperature, T_{max}, measured at the surface of the weld site is given for each set of parameters. The average change in temperature, ΔT, is the peak radiometric surface temperature during the 61st laser pulse minus the lowest temperature to which the tissue cooled between the 60th and 61st pulses. If one compares the T_{max} columns of data for the in vitro set of parameters, it can be concluded that longer cooling times result in lower peak temperatures for all three positions at the tissue surface. Within each row of data, ΔT decreases as the temperature is measured farther from the weld site. Preferential absorption of the laser radiation at the incision site causes a large temperature rise near the incision. The associated thermal gradient leads to rapid cooling near the incision and thus the large on-axis ΔT.

DISCUSSION

The in vitro temperature data show several trends. First, short and intermediate interpulse cooling times (τ_c = 1.6 and 4.0 seconds) did not allow sufficient cooling of the weld site between successive pulses of radiation. Insufficient cooling resulted in a buildup of heat in the tissue as shown by the continual increase of both the peak and baseline temperatures over the span of 70 pulses, until peak temperatures reached over 100°C on axis for τ_c = 1.6 seconds.

For short and intermediate cooling times, baseline temperatures rose above the thermal damage threshold (~65°C) for extended periods, effectively creating a CW welding mode. During welding with these cooling times, heat diffused out of the weld site into the surrounding tissue, resulting in a significant amount of thermal damage [1]. For example, for short cooling durations of 1.6 seconds, the temperature as far as 6 mm away from the weld site reached as high as 60°C. Previous histologic studies using these parameters have shown that acute thermal denaturation near the epidermis extended to 2.7 ± 0.3 mm from the axis of the weld site after the application of 70 laser scans [1]. The extent of thermal denaturation near the epidermis was also large for the 4-second cooling studies, measuring 1.4 ± 0.5 mm
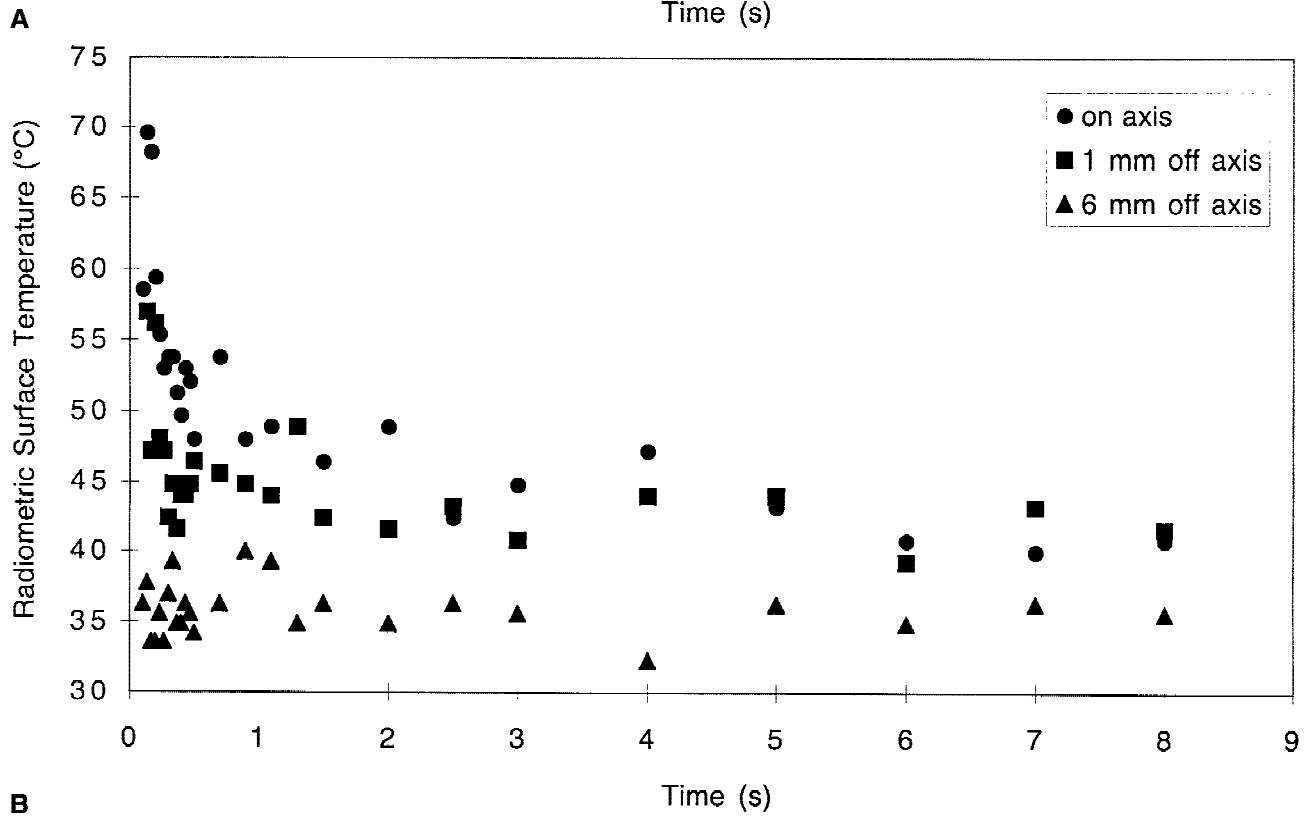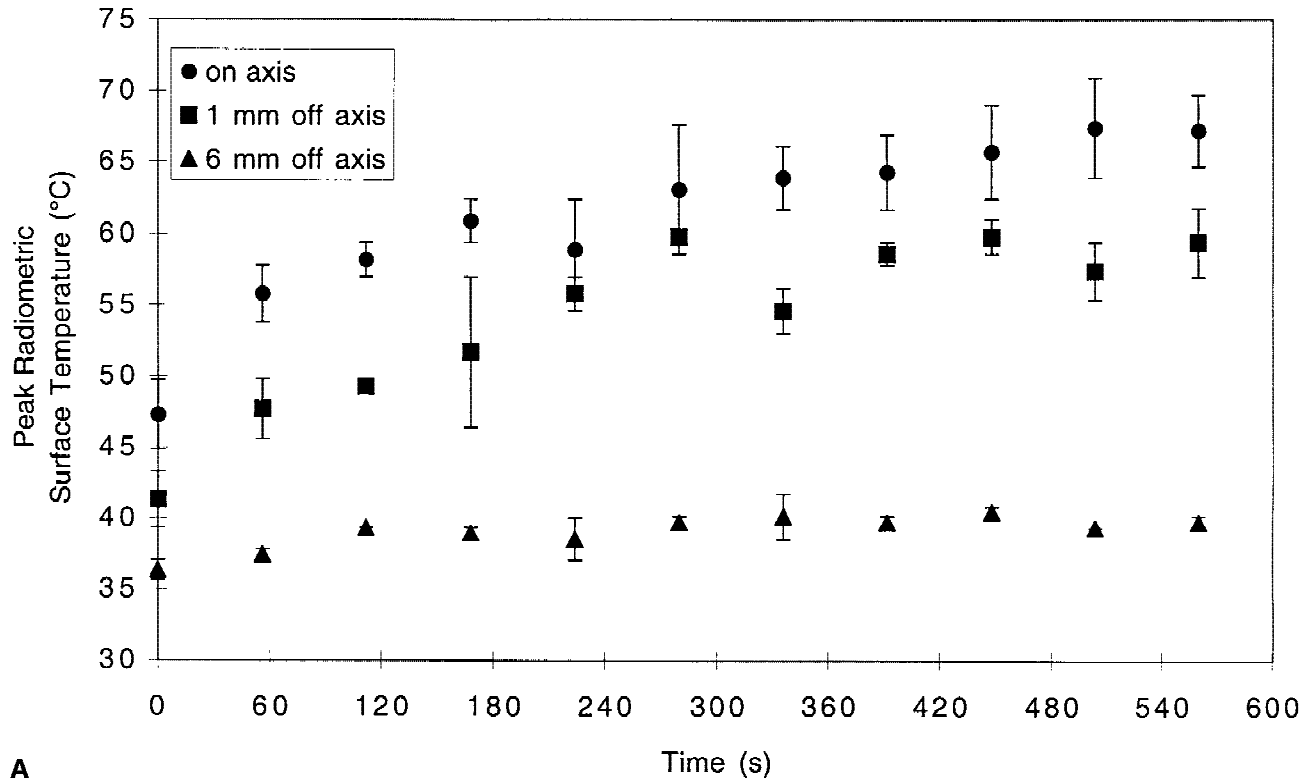
Fig. 5. **A:** Peak radiometric surface temperatures for welding in vivo as a function of time and distance from the weld site for 8 seconds of cooling between scans. Bars signify mean values ± SD (n = 2). **B:** Time–temperature profile for welding in vivo during the 61st scan with 8 seconds of cooling between scans.

TABLE 2. Summary of the Temperature Measurements*

Study	On axis		1 mm off axis		6 mm off axis	
	T_{max}	ΔT	T_{max}	ΔT	T_{max}	ΔT
In vitro						
$\quad \tau_c = 1.6$ sec	104 ± 6	24 ± 3	97 ± 14	17 ± 4	61 ± 6	8 ± 2
$\quad \tau_c = 4.0$ sec	88 ± 1	28 ± 1	78 ± 4	21 ± 2	54 ± 3	8 ± 1
$\quad \tau_c = 8.0$ sec	59 ± 1	16 ± 3	52 ± 1	10 ± 2	43 ± 3	8 ± 1
In vivo						
$\quad \tau_c = 8.0$ sec	69 ± 2	24 ± 2	60 ± 3	19 ± 2	40 ± 1	7 ± 1

*τ_c, cooling time; T_{max}, maximum temperature (°C); ΔT, average change in temperature (°C).

from the axis of the weld site, after the application of 70 laser scans [1]. Thus, heating of the tissue was clearly not confined to the targeted 200-μm-wide zone around the weld site.

By providing sufficient cooling of the weld site between pulses ($\tau_c = 8.0$ seconds), temperatures above the thermal denaturation threshold were reached for short periods (~100 msec), whereas baseline temperatures remained low. The peak temperatures were confined to the immediate area of the weld site, producing selective cumulative thermal denaturation and reducing unnecessary thermal damage to healthy tissue surrounding the weld site. Previous histologic studies using these parameters have shown an acute lateral thermal denaturation zone of 500 ± 150 μm near the epidermis, with less than 200 μm of lateral thermal denaturation in the middle and bottom layers of the dermis, when using a total of 35 laser pulses [1].

The in vivo temperature data taken for long cooling times between pulses ($\tau_c = 8.0$ seconds) show results similar to those of the in vitro measurements. The peak surface temperature measurements were higher in vivo (69°C) than in vitro (59°C). However, this difference was due to the higher fluences used for the in vivo experiments (6.7 J/cm^2) than for the in vitro experiments (5.1 J/cm^2). Otherwise, similar trends were noted: surface temperatures rose to approximately the thermal denaturation threshold for short periods of time (~100 msec) and then cooled well below the threshold. These elevated temperatures were confined to the weld site. Previous histologic studies using these parameters produced a thermal denaturation zone of only 200 ± 40 μm near the epidermis, with thermal denaturation extending only approximately 1 mm in depth [2].

A reasonable explanation exists for the finding that in vitro surface temperatures of only ~60°C produced ~2-mm-deep welds, whereas in vivo temperatures of ~70°C produced only ~1-mm deep welds. The absence of blood flow and de-creased hydration in vitro probably resulted in subsurface temperatures higher than would be achieved with the same parameters in vivo. Blood flow and hydration of the tissue serve to draw heat away from the weld site through convection and conduction, respectively. These phenomena probably resulted in a large temperature gradient with depth in vivo, in turn resulting in a large gradient in the thermal denaturation. Thus, a much higher surface temperature is necessary in vivo to produce the same subsurface temperatures as achieved in vitro. It should be emphasized that, although only surface temperatures were recorded in this study, subsurface temperature measurements on the axis of the weld site would be necessary to verify this explanation.

Surface temperatures much higher than 70°C will be necessary to achieve temperatures above the thermal denaturation threshold in the deepest layers of the dermis. Deeper denaturation of the tissue can be achieved by delivering fluences higher than those used in this study. A pulse duration significantly shorter than 100 msec will also be necessary to further confine heating to the weld site and reduce the temperature rise in the surrounding tissue. For example, peak temperatures measured at 1 mm from the weld site reached as high as 60°C in the in vivo studies. The rise time in surface temperature will be a function of the pulse duration, local absorption coefficient, fluence, and thermal properties of the tissue, and the decay time will be a function of the thermal properties of the tissue and its geometry. Thus, by shortening the pulse duration, heating will be further confined to the weld site and the extent of thermal damage in surrounding tissue will be decreased.

The relatively large standard deviations seen in all of the temperature measurements should be discussed. The deviations in the data are not primarily the result of limitations of the thermal camera. It is known that the thermal camera will underestimate the temperature of

small targets or targets in which there are axial temperature gradients [14]. In this application, the pulse duration, τ_p, is ~100 msec. At an image capture rate of 33 msec, the camera should capture the approximate peak temperature of the tissue. With an absorption coefficient, μ_a, of 3,500 cm^{-1} for the India ink [1], one calculates an effective penetration depth for the radiation of ~3 μm. Because the width of the ink layer (40–100 μm) is much greater than the effective penetration depth in the India ink, thermal diffusion should occur axially in the tissue first. The thermal diffusivity of skin, κ, is approximately 1.4×10^{-3} cm^2/sec [15]. Therefore, the thermal relaxation time in the ink-stained tissue is calculated to be $\tau_r = d^2/4\kappa = 15$ μsec. Because $\tau_p \gg \tau_r$, significant thermal diffusion occurs during the laser pulse, which will lead to a slight underestimation of the actual surface temperature. Because the time between images (33 msec) is much longer than the thermal relaxation time, however, the averaging of temperature measurements should theoretically result in small standard deviations in the data.

The errors in measurement are more likely due to a nonuniform staining of the weld site, which resulted in the occurrence of "hot spots" in the tissue. These hot spots are probably due to a combination of several factors including a variation in dye uptake in the tissue and the presence of fluids such as blood and water at the weld site, which may wash away some of the dye. The hot spots in turn resulted in large temperature variations along the surface of the ink layer and made averaging of multiple samples a necessity. Animal breathing in the in vivo experiments probably had a small but significant effect on the variation of fluence at the weld site and on the positions at which temperatures were recorded.

It should be stated that the thermal damage threshold of ~65°C for skin was used as a reference in this study. This temperature was determined based on previous studies that applied an Arrhenius thermal damage model to the heating of tissue. There are several major limitations, however, to using an Arrhenius thermal damage model to determine thermal damage in this study. First, lack of knowledge of the rate process parameters for this application limits a comprehensive analysis. Second, the model assumes that the temperature is constant over the heating duration, which is not the case in this tissue welding technique because radiation is delivered to the tissue in a pulsed mode, thus creating transient temperatures. Third, the model predicts accumulation of thermal damage over a single heating period. In this application, however, thermal damage accumulates slowly through the application of multiple pulses of radiation. Fourth, the assumption of the model that tissue denaturation follows first-order reaction kinetics is questionable [16,17]. For these reasons, no attempt was made to rigorously apply the Arrhenius model to predict thermal denaturation from the temperatures measured in this study. Instead, the objective was to correlate temperature measurements with thermal damage zones at the weld site that were measured in previous studies [1–2].

CONCLUSIONS

In summary, the temperature measurements demonstrate that short ($\tau_c = 1.6$ seconds) and intermediate ($\tau_c = 4.0$ seconds) cooling times between laser pulses were not long enough to produce sufficient cooling of the tissue surface to temperatures significantly below the thermal damage threshold between pulses. Tissue temperatures continued to increase, approaching 100°C on the axis of the weld site, with successive pulses. The net effect was that the tissue temperatures remained above the thermal damage threshold for prolonged periods, in a similar manner to welding in a CW mode, resulting in excessive thermal damage to surrounding tissue.

Long cooling times between pulses ($\tau_c = 8.0$ seconds) were necessary to prevent a buildup of the baseline temperature above the thermal damage threshold. Selective and cumulative thermal denaturation of the weld site was achieved while preventing unnecessary thermal damage to adjacent tissue. Higher fluences and shorter pulse durations than currently used in this study, however, will be necessary to achieve thermal denaturation in the deepest layers of the dermis and to limit heating of tissue immediately surrounding the weld site, respectively.

This study provides further evidence that it is possible to cause selective thermal denaturation at the weld site without overheating adjacent tissue if the laser energy is delivered in a pulsed mode with sufficiently short pulse durations and adequate cooling times between applications of successive pulses. Thus, this mode of energy delivery represents a promising alternative to current welding techniques that use CW delivery of radiation and/or active temperature-controlled feedback systems.

REFERENCES

1. Fried NM, Walsh JT. Dye-assisted laser skin closure with pulsed radiation: an in vitro study of weld strength and thermal damage. J Biomed Optics 1998;3:401–408.
2. Fried NM, Walsh JT. Dye-assisted laser skin welding with pulsed radiation: in vivo wound healing results. Lasers Surg Med 1998;Suppl 10:48.
3. Robinson JK, Garden JM, Taute PM, Leibovich SJ, Lautenschlager EP, Hartz RS. Wound healing in porcine skin following low-output carbon dioxide laser irradiation of the incision. Ann Plast Surg 1987;18:499–505.
4. Garden JM, Robinson JK, Taute PM, Lautenschlager EP, Leibovich SJ, Hartz RS. The low-output carbon dioxide laser for cutaneous wound closure of scalpel incisions: comparative tensile strength studies of the laser to the suture and staple for wound closure. Lasers Surg Med 1986;6:67–71.
5. Abergel RP, Lyons R, Dwyer R, White RR, Uitto J. Use of lasers for closure of cutaneous wounds: experience with Nd:YAG, argon, and CO_2 lasers. J Dermatol Surg Oncol 1986;12:1181–1185.
6. Dew DK, Hsu TM, Halpern SJ, Michaels CE. Laser assisted skin closure at 1.32 microns: The use of a software driven medical laser system. Proc SPIE 1991;1422:111–115.
7. Wider TP, Libutti SK, Greenwald DP, Oz MC, Yager JS, Treat MR, Hugo NE. Skin closure with dye-enhanced laser welding and fibrinogen. Plast Reconstr Surg 1991;88:1018–1025.
8. Poppas DP, Stewart RB, Massicotte JM, Wolga AE, Kung RTV, Retik AB, Freeman MR. Temperature-controlled laser photocoagulation of soft tissue: in vivo evaluation using a tissue welding model. Lasers Surg Med 1996;18:335–344.
9. Moritz AR, Henriques FC. Studies of thermal injury II. The relative importance of time and surface temperature in the causation of cutaneous burns. Am J Pathol 1947;23:695–720.
10. Weaver JA, Stoll AM. Mathematical model of skin exposed to thermal radiation. Aerospace Med 1969;40:24–30.
11. Walsh JT. Pulsed laser ablation of tissue: analysis of the removal process and tissue healing [PhD thesis]. Cambridge: Massachusetts Institute of Technology; 1988. p 202–257.
12. Green HA, Burd EE, Nishioka NS, Compton CC. Skin graft take and healing following 193 nm excimer, continuous-wave carbon dioxide (CO_2), or pulsed holmium:YAG laser ablation of the graft bed. Arch Dermatol 1993;129:979–988.
13. Pearce JA, Welch AJ, Motamedi M, Agah R. Thermographic measurement of tissue temperature during laser angioplasty. In: Diller KR, Roemer RB, eds. Heat and mass transfer in the microcirculation of thermally significant vessels. New York: ASME; 1986.
14. Torres JH, Springer TA, Welch AJ, Pearce JA. Limitations of a thermal camera in measuring surface temperature of laser-irradiated tissues. Lasers Surg Med 1990;10:510–523.
15. Bowman HF, Cravalho EG, Woods M. Theory, measurement, and application of thermal properties of biomaterials. Annu Rev Biophys Bioeng 1975;4:43–80.
16. Maitland DJ, Walsh JT. Quantitative measurements of linear birefringence during heating of native collagen. Lasers Surg Med 1997;20:310–318.
17. Sankaran V, Walsh JT. Birefringent measurement of rapid structural changes during collagen denaturation. Photochem Photobiol 1998;68:846–851.